

## Protein Assistance in the Photoisomerization of Rhodopsin and 9-*cis*-Rhodopsin—Insights from Experiment and Theory

Sivakumar Sekharan,<sup>†</sup> Minoru Sugihara,<sup>†</sup> Oliver Weingart,<sup>†</sup> Tetsuji Okada,<sup>\*,‡</sup> and Volker Buss<sup>\*,†</sup>

Departments of Chemistry and Physics, University of Duisburg-Essen, 47048 Duisburg, Germany, and Biological Information Research Center, National Institute of Advanced Industrial Science and Technology, AIST 2-41-6 Aomi, Koto-ku, Tokyo 135-0064, Japan

Received October 26, 2006; E-mail: volker.buss@uni-due.de; t-okada@aist.go.jp

11-*cis*-Retinal protonated Schiff base (pSb11) is the chromophore of rhodopsin that mediates the first step in the process of vision: after excitation by a 500 nm photon the chromophore isomerizes in an ultrafast and highly efficient reaction to all-*trans*- or bathorhodopsin. The energy captured in this process is used to drive the protein through a sequence of intermediates which finally activates the visual cascade and excites the optic nerve.<sup>1</sup> Recent years have seen considerable progress in understanding structure–function relationships in retinal binding proteins; however, the factors responsible for the most remarkable photochemistry of these systems are still a matter of debate.

9-*cis*-Retinal protonated Schiff base, pSb9, is the chromophore of 9-*cis*-rhodopsin, a rhodopsin analogue that photoisomerizes to the same intermediate, bathorhodopsin, though in a reaction which is at the same time slower and less efficient.<sup>2</sup> Advances in the preparation of rhodopsin crystals containing pSb9<sup>3</sup> have afforded a close-up view of how the artificial chromophore is accommodated inside the rhodopsin binding pocket.<sup>4</sup> Together with the crystal structure of rhodopsin<sup>5–7</sup> this provides the first opportunity to carry out a comparative study on the structure and the primary photo-reaction of rhodopsin and 9-*cis*-rhodopsin. Here we use the results from X-ray crystallography and from quantum-mechanical calculations to study how the protein shapes the retinal chromophore and assists in bringing about its unique photochemistry.

The theoretical model of 9-*cis*-rhodopsin that we use in this study was obtained in a procedure described in detail elsewhere.<sup>8</sup> In short, starting with the quantum-mechanically optimized rhodopsin binding pocket consisting of the chromophore, 28 nearest amino acid residues and two water molecules,<sup>6</sup> the chromophore, pSb11 was replaced by pSb9, and the complete pocket was reoptimized. The experimental model was obtained from the recent crystallographic study of artificial rhodopsin crystals containing 9-*cis*-rhodopsin. For this model we used the same set of starting parameters (bond lengths, bond angles, and dihedral angles) as applied previously to native rhodopsin<sup>6</sup> except for the two dihedral angles around the C9=C10 and C11=C12 bonds. The resulting chromophore geometries are compared in Figure 1.

Bond length alternation along the conjugated polyene chain is weaker in the theoretical compared to the experimental structure, which is commonly observed in calculations that include electron correlation.<sup>8</sup> Also, the experimental model appears biased toward relaxing strain energy by adjusting bond angles along the chain, especially around the C7=C8 bond. However, the dihedral angles are reproduced very well; note the C6–C7 dihedral which reflects the *cis* orientation of the  $\beta$ -ionone ring, and in particular the negative twist of the C9=C10 double bond (calcd,  $-9^\circ$ ; exptl,  $-10^\circ$ ).

To evaluate the significance of the differences between experi-

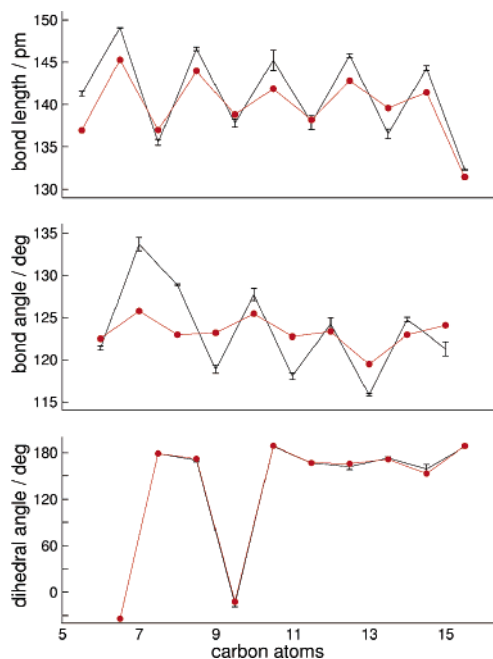


**Figure 1.** Comparison between the calculated (in red) and the X-ray structure (in black) of the chromophore in 9-*cis*-rhodopsin. Experimental values come in doubles corresponding to molecules A and B of the asymmetric unit.

ment and theory, we carried out a second crystallographic refinement using the same diffraction data as above and the set of initial retinal parameters obtained from the quantum mechanical study of the 9-*cis*-rhodopsin chromophore. The refinement of this retinal structure results in a better agreement of bond lengths and bond angles with the quantum mechanical model (see Supporting Information, Table T1), which demonstrates that these parameters are affected by the choice of starting values at the current experimental resolution. Which of the two refinements is likely to be realistic is not an issue to be examined here. However, the differences (atomic displacements) between the two crystallographic structures are found to be negligible, as shown in Figure 2. This comparison indicates that small uncertainties in bond lengths and bond angles affect neither the shape of the chromophore nor the distances of each atom to the nearby protein atoms.

The pretwist of the isomerizing *cis*-double bond is probably a prerequisite for the fast and efficient photoreaction of rhodopsins. From a study of several rhodopsin analogues differing in the methyl substitution pattern of the 11-*cis*-retinal chromophore, Mathies and Lugtenburg concluded that rhodopsin provides a dramatic example for the role of ground-state conformational control in a photochemical reaction.<sup>1</sup> This control is achieved through the induced fit of

<sup>†</sup> University Duisburg-Essen at Duisburg.

<sup>‡</sup> AIST.

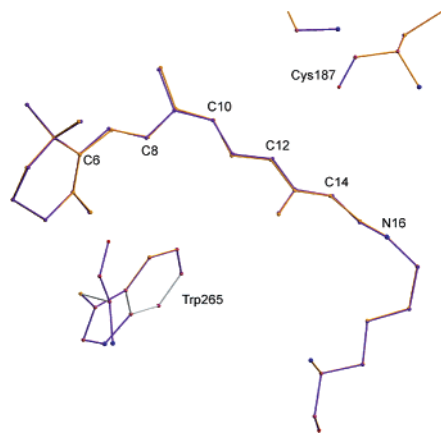


**Figure 2.** Overlay of the two 9-*cis*-rhodopsin models obtained from conjugate gradient minimization of the X-ray model using two different sets of initial parameters for the chromophore: purple, from crystallography; yellow, from quantum mechanics (see text).

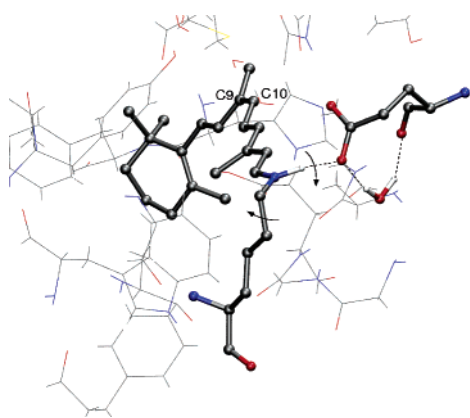


**Figure 3.** The pSb9 chromophore inside the 9-*cis*-rhodopsin binding pocket. The covalently attached Lys296 and the counterion Glu113 are seen to exert a clockwise torque on the plane of the N16 fragment leading to the negative twist of the C9=C10 bond.

the chromophore in the binding pocket. With the two ends of the retinal pSb fixed by the protein—the  $\beta$ -ionone ring inside a hydrophobic binding pocket and the Schiff base nitrogen by covalent binding with Lys296 and the salt bridge to Glu113—the carbon chain is left to bridge the distance under the constraint of preserving maximum planarity along the conjugated double bonds.

In rhodopsin, this divides the chromophore chain into two almost planar entities, from C7 to C11 and from C12 to N16, which meet under different angles at the C11=C12 double bond. The twist thus induced in this bond is supported by the C13 methyl group.<sup>9</sup> In 9-*cis*-rhodopsin, the situation is analogous (Figure 3), however, the twist angle of the C9=C10 bond is smaller possibly because of the missing methyl group. This may be one of the reasons for the small activation barrier observed for the photoisomerization of 9-*cis*-rhodopsin<sup>10</sup> and for the inferior photoreceptor properties, comparable to the less effective photoreaction of 13-demethylrhodopsin,<sup>11,12</sup> relative to rhodopsin.

A second consequence of the induced fit of the chromophore in the binding pocket is the sense in which the *cis*-double bond is twisted. The sense is positive leading to a negative dihedral angle in both rhodopsin and 9-*cis*-rhodopsin (see Figure 3). Spectral manifestation of this sign is the circular dichroism (CD) of the optical transition ( $\alpha$ -band) which is positive in rhodopsin and 9-*cis*-rhodopsin, but somewhat smaller in magnitude in the latter.<sup>13</sup> It is interesting to note that the CD of the  $\alpha$ -band of several rhodopsin analogues with different methyl substitution patterns at the 10- and

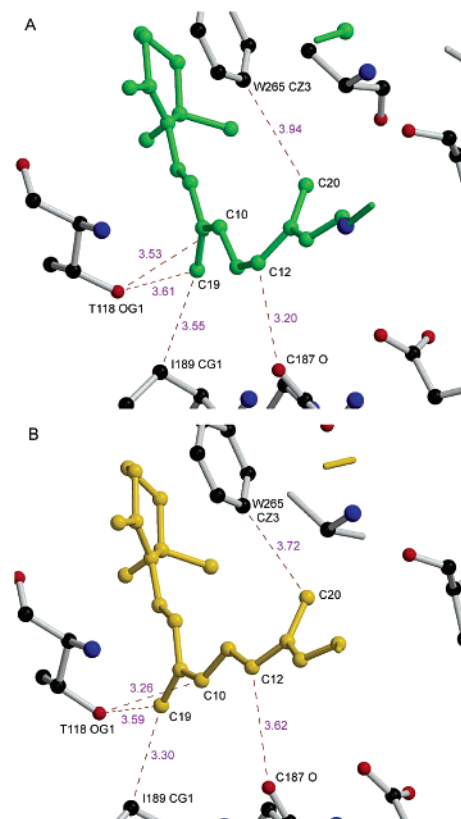


**Figure 4.** Differences in the retinal-protein interactions between rhodopsin (upper) and 9-*cis*-rhodopsin (lower). Distances (Å) between the atoms are shown in yellow for one of the two molecules in the asymmetric unit.

13-14 and at the 14-position<sup>15</sup> has been found to be positive throughout, another indication that the global chromophore conformation is determined by the induced fit of its end groups.

Next we examine the differences in the interaction of retinal with the surrounding protein atoms (Figure 4). The positions of retinal polyene carbons differ especially at C10, C11, and C12 between 11-*cis* and 9-*cis* forms. In rhodopsin, the closest atom to the 11-*cis*-retinal chromophore is the peptide oxygen of Cys187 in the second extracellular loop. This atom is supposed to assist the large dislocation of C12 during isomerization by repulsive interaction.<sup>16</sup> We have carefully examined the deviation of this distance by taking eight values from the four coordinate files (PDB ID: 1F88, 1HZX, 1L9H, 1U19) of the tetragonal rhodopsin crystal and obtained an average of 3.13 Å. With regard to this specific interaction, it should be noted that the distance between the oxygen of Cys187 and C12 is longer in 9-*cis*-rhodopsin (3.62 and 3.61 Å for the two molecules in the asymmetric unit). In accord with this change, isomerization of 9-*cis*-retinal does not require as large displacement of C12 as rhodopsin.

On the other hand, the distance between C10 and the side chain oxygen of Thr118 is shorter in 9-*cis*-rhodopsin (3.31 Å, average from two models) than in rhodopsin (3.64 Å, averaged from eight models). This close interaction must be critical for the large movement of C10 during photoisomerization of 9-*cis*-rhodopsin because no other protein atoms are present within 4 Å from C10. From these observations, it appears possible that the protein may assist the photoisomerization process of the two isomers via different oxygen atoms, carbonyl oxygen of C187 for rhodopsin and the side chain oxygen of Thr118 for 9-*cis*-rhodopsin.

Another substantial change of distance can be seen between C19 and Ile189 CG1 (3.28 Å in 9-*cis*-rhodopsin and 3.70 Å in

**Table 1.** CASPT2 Energies and Oscillator Strengths of 11-*cis* and 9-*cis*-Retinal Protonated Schiff Base in Different Environments<sup>a</sup>

model	state	pSb11		pSb9	
		CASPT2 <sup>b,d</sup>	<i>f</i>	CASPT2 <sup>c,d</sup>	<i>f</i>
vac	S <sub>0</sub>	-871.2306		-4.0	
	S <sub>1</sub>	47.3 ( <b>606</b> )	1.12	48.2 ( <b>593</b> )	1.05
	S <sub>2</sub>	65.5 (436)	0.13	68.2 (419)	0.18
dist	S <sub>0</sub>	-871.2185		-3.4	
	S <sub>1</sub>	44.5 ( <b>643</b> )	0.96	46.3 ( <b>617</b> )	1.00
	S <sub>2</sub>	63.9 (447)	0.14	66.4 (431)	0.16
ip	S <sub>0</sub>	-1060.0803		+0.6	
	S <sub>1</sub>	58.8 ( <b>486</b> )	0.82	60.0 ( <b>477</b> )	0.84
	S <sub>2</sub>	67.6 (423)	0.00	70.1 (408)	0.00
pe	S <sub>0</sub>	-1060.7835		+3.9	
	S <sub>1</sub>	57.0 ( <b>502</b> )	0.79	58.3 ( <b>490</b> )	0.80
	S <sub>2</sub>	67.6 (429)	0.00	69.2 (413)	0.00

<sup>a</sup> Wavelengths of the allowed optical transition (in nm) are given in bold font. See text for abbreviations. <sup>b</sup> S<sub>0</sub> energies in au. <sup>c</sup> S<sub>0</sub> energies relative to the corresponding S<sub>0</sub> energy of pSb11, in kcal·mol<sup>-1</sup>. <sup>d</sup> S<sub>1</sub> and S<sub>2</sub> energies relative to S<sub>0</sub> in kcal·mol<sup>-1</sup>.

rhodopsin). This is in line with the larger movement of C19 in 9-*cis*-rhodopsin compared to rhodopsin. Thus, we suppose that Thr118 and Ile189 assist the photoisomerization in 9-*cis*-rhodopsin, although the location of these closest atoms relative to the direction of atomic movement of the interacting carbon of retinal upon excitation does not appear to be as favorable as in rhodopsin (Cys187 O and C12).

These structural analyses of 9-*cis*-rhodopsin are supported by quantum-mechanical calculations of the UV–vis spectral data and of the ground-state energy of the chromophore inside the protein pocket. These data, which are obtained on the basis of the quantum-mechanical model, reveal a close correlation with corresponding data for the natural chromophore.

We have shown recently that the 498 nm absorption maximum of rhodopsin can be reproduced with high accuracy using multi-configurational CASSCF methodology combined with second-order perturbation theory (CASPT2).<sup>17</sup> In addition to the quantum-mechanical description for the chromophore and its counterion we used atomic charges obtained from a natural population analysis to account for the electrostatic interaction between the chromophore and the polar amino acids. The data shown in Table 1 under “pSb11” reveal how the absorption of the bare chromophore (“vac”) at 606 nm is red-shifted to 643 nm because of the distortions induced by the protein (“dist”). Ion-pairing (“ip”) with Glu113 moves the absorption close to the experimental value, while the additional charges from the amino acid residues mimicking the protein-embedded chromophore (“pe”) produce only a small red-shift of 16 nm.

The conclusions drawn from that study—that the spectrum of rhodopsin is primarily determined by the counterion—holds true for 9-*cis*-rhodopsin as well, as perusal of the table shows. Chromophore distortion and the amino acid charges produce red-shifts of 24 and 13 nm, respectively, while the counterion induced blue-shift is 140 nm. The resulting absorbance, 490 nm, is in very good agreement with the experimental value of 485 nm.<sup>18</sup> The 13 nm blue-shift (calcd, 12 nm) of 9-*cis*-rhodopsin relative to rhodopsin can be traced back to the less distorted chromophore in vacuo (the relaxed pSb9 chromophore is essentially planar) and the significantly smaller red-shift suffered through distortion by the protein pocket, a consequence of steric misfit in the binding site of 9-*cis*-rhodopsin.<sup>19</sup>

The calculated ground state energies agree with this analysis. pSb9<sub>vac</sub> is lower in energy than pSb11<sub>vac</sub> by 4 kcal·mol<sup>-1</sup> for reasons

discussed above. The gap decreases insignificantly to 3.4 kcal·mol<sup>-1</sup>. Inclusion of the counterion and, finally, the protein charges reverse the stability, in agreement with photocalorimetric measurements on the two pigments<sup>20,21</sup> which place the 9-*cis*-isomer some 5 kcal·mol<sup>-1</sup> above rhodopsin.

In conclusion, the present study provides a possible explanation for the relation between the photoreactivity and the protein assistance and gives insights to manipulating the sophisticated biological function. It has highlighted the key role which the binding pocket plays in shaping and thus preparing the chromophore for the upcoming photochemical event.

**Acknowledgment.** This research was supported in Japan by grants from MEXT and NEDO and in Germany by the DFG (Forschergruppe Retinal Protein Action).

**Supporting Information Available:** Details of the computational setup, a table comparing internal coordinates from refined and quantum-mechanical models, and Cartesian coordinate files of all systems discussed in this study. This material is available free of charge via the Internet at <http://pubs.acs.org>.

## References

- Mathies, R. A.; Lugtenburg, J. In *Molecular Mechanisms of Visual Transduction*; Stavenga, D. G., DeGrip, W. J., Pugh, E. N., Jr., Eds.; Elsevier: Amsterdam, The Netherlands, 2000; p 55.
- Schoenlein, R. W.; Peteanu, L. A.; Wang, Q.; Mathies, R. A.; Shank, C. V. *J. Phys. Chem.* **1993**, *97*, 12087.
- Okada, T.; Tsujimoto, R.; Muraoka, M.; Funamoto, C. In *G Protein-Coupled Receptors: Structure, Function and Ligand Screening*; Haga, T., Takeda, S., Eds.; CRC Press: Boca Raton, FL, 2005; pp 245.
- Nakamichi, H.; Okada, T. *Photochem. Photobiol.*, published online, <http://dx.doi.org/10.1562/2006-06-13-RA-920>.
- Palczewski, K.; Kumasaka, T.; Hori, T.; Behnke, C. A.; Motoshima, H.; Fox, B. A.; LeTrong, I.; Teller, D. C.; Okada, T.; Stenkamp, R. E.; Yamamoto, M.; Miyano, M. *Science* **2000**, *289*, 739.
- Okada, T.; Sugihara, M.; Bondar, A.-N.; Elstner, M.; Entel, P.; Buss, V. *J. Mol. Biol.* **2004**, *342*, 571.
- Li, J.; Edwards, P. C.; Burghammer, M.; Villa, C.; Schertler, G. F. *J. Mol. Biol.* **2004**, *343*, 1409.
- Sugihara, M.; Buss, V.; Entel, P.; Elstner, M.; Frauenheim, T. *Biochemistry* **2002**, *41*, 15259.
- Sugihara, M.; Hufen, J.; Buss, V. *Biochemistry* **2006**, *45*, 801.
- Birge, R. B.; Einterz, C. M.; Knapp, H. M.; Murray, L. P. *Biophys. J.* **1988**, *53*, 367.
- Kochendoerfer, G. G.; Verdegem, P. J. E.; van der Hoef, I.; Lugtenburg, J.; Mathies, R. A. *Biochemistry* **1996**, *35*, 16230.
- Koch, D.; Gärtner, W. *Photochem. Photobiol.* **1997**, *65*, 181.
- Burke, M. J.; Pratt, D. C.; Faulkner, T. R.; Moscovitz, A. *Exp. Eye Res.* **1973**, *17*, 557.
- DeLange, F.; Bovee-Geurts, P. H. M.; VanOostrum, J.; Portier, M. D.; Verdegem, P. J. E.; Lugtenburg, J.; DeGrip, W. J. *Biochemistry* **1998**, *37*, 1411.
- Ebrey, T.; Govindjee, R.; Honig, B.; Pollock, E.; Chan, W.; Crouch, R.; Yudd, A.; Nakanishi, K. *Biochemistry* **1975**, *14*, 3933.
- Liu, R. S. H.; Hammond, G. S. *Acc. Chem. Res.* **2005**, *38*, 396.
- Sekharan, S.; Sugihara, M.; Buss, V. *Angew. Chem., Int. Ed.* **2007**, *46*, 269.
- Spalink, J. D.; Reynolds, A. H.; Rentzepis, P. M.; Sperling, W.; Applebury, M. L. *Proc. Natl. Acad. Sci. U.S.A.* **1983**, *80*, 1887.
- Creemers, A. F. L.; Bovee-Geurts, P. H. M.; DeGrip, W. J.; Lugtenburg, J.; de Groot, H. H. M. *Biochemistry* **2004**, *43*, 16011.
- Cooper, A. *FEBS Lett.* **1979**, *100*, 382.
- Schick, G. A.; Cooper, T. M.; Holloway, R. A.; Murray, L. P.; Birge, R. R. *Biochemistry* **1987**, *26*, 2556.

JA066970P